



**HAL**  
open science

## Secondary structure and $^1\text{H}$ , $^{15}\text{N}$ & $^{13}\text{C}$ resonance assignments of the periplasmic domain of OutG, major pseudopilin from *Dickeya dadantii* type II secretion system

Theis Jacobsen, Régine Dazzoni, Melvin Renault, Benjamin Bardiaux, Michael Nilges, Vladimir Shevchik, Nadia Izadi-Pruneyre

### ► To cite this version:

Theis Jacobsen, Régine Dazzoni, Melvin Renault, Benjamin Bardiaux, Michael Nilges, et al.. Secondary structure and  $^1\text{H}$ ,  $^{15}\text{N}$  &  $^{13}\text{C}$  resonance assignments of the periplasmic domain of OutG, major pseudopilin from *Dickeya dadantii* type II secretion system. *Biomolecular NMR Assignments*, 2022, 16 (2), pp.231-236. 10.1007/s12104-022-10085-4. hal-03836613

**HAL Id: hal-03836613**

**<https://hal.science/hal-03836613v1>**

Submitted on 16 Nov 2022

**HAL** is a multi-disciplinary open access archive for the deposit and dissemination of scientific research documents, whether they are published or not. The documents may come from teaching and research institutions in France or abroad, or from public or private research centers.

L'archive ouverte pluridisciplinaire **HAL**, est destinée au dépôt et à la diffusion de documents scientifiques de niveau recherche, publiés ou non, émanant des établissements d'enseignement et de recherche français ou étrangers, des laboratoires publics ou privés.



Distributed under a Creative Commons Attribution 4.0 International License

1 **Secondary structure and<sup>1</sup>H, <sup>15</sup>N & <sup>13</sup>C resonance assignment of**  
2 **the periplasmic domain of OutG, major pseudopilin from**  
3 ***Dickeya dadantii* type II secretion system**

4 Theis Jacobsen<sup>1</sup>, Régine Dazzoni<sup>1</sup>, Melvin Renault<sup>2,3</sup>, Benjamin Bardiaux<sup>1</sup>, Michael Nilges<sup>1</sup>,  
5 Vladimir Shevchik<sup>2,3</sup>, Nadia Izadi-Pruneyre<sup>1\*</sup>

6  
7 1: Institut Pasteur, Université de Paris, CNRS UMR3528, Structural Bioinformatics Unit, F-  
8 75015 Paris, France 2: Université de Lyon 1, INSA-Lyon, F-69621 Villeurbanne, France.  
9 3: CNRS, UMR5240, Microbiologie Adaptation et Pathogénie, F-69622 Lyon, France.

10  
11 \* corresponding author: [nadia.izadi@pasteur.fr](mailto:nadia.izadi@pasteur.fr)

12  
13 **Declarations**

14 Keywords: NMR resonance assignment, Type II Secretion System, OutG, *Dickeya dadantii*,  
15 pseudopilin

16 **Funding**

17 This work was funded by the Institut Pasteur, the Centre National de la Recherche Scientifique  
18 (CNRS), the French Agence Nationale de la Recherche (ANR Synergy-T2SS ANR-19-CE11-  
19 0020-01) and European Union's Horizon 2020 Research and Innovation program under the  
20 Marie Skłodowska-Curie Grant agreement no 765042. The 800-MHz NMR spectrometer of the  
21 Institut Pasteur was partially funded by the Région Ile de France (SESAME 2014 NMRCHR  
22 grant no 4014526).

23  
24 **Conflicts of interest/Competing interests**

25 The authors declare they have no conflict of interest.

26  
27 **Availability of data and material (data transparency)**

28 The chemical shift values have been deposited in the BioMagResBank  
29 (<http://www.bmrb.wisc.edu/>) under the accession number 51296.

30

31

32 Code availability (software application or custom code) Not applicable.

33

34 Ethics approval

35 The experiments comply with the current laws of France.

36 The corresponding author, Nadia Izadi-Pruneyre, serves as guarantor for the article and accepts  
37 full responsibility for the work and the conduct of the study.

38

39 All authors:

40 1) made substantial contributions to the conception or design of the work; or the acquisition,  
41 analysis, or interpretation of data;

42 2) drafted the work or revised it critically for important intellectual content;

43 3) approved the version to be published; and

44 4) agree to be accountable for all aspects of the work in ensuring that questions related to the  
45 accuracy or integrity of any part of the work are appropriately investigated and resolved

## 46 **Abstract**

47 Abstract length: 189 words.

48 The ability to interact and adapt to the surrounding environment is vital for bacteria that  
49 colonise various niches and organisms. One strategy developed by Gram-negative bacteria is  
50 to secrete exoprotein substrates *via* the type II secretion system (T2SS). The T2SS is a  
51 proteinaceous complex spanning bacterial envelope that translocates folded periplasmic  
52 proteins such as toxins and enzymes to the extracellular milieu. In T2SS, a cytoplasmic ATPase  
53 elongates in the periplasm the pseudopilus, a non-covalent polymer composed of protein  
54 subunits named pseudopilins, anchored in the inner membrane by a transmembrane helix. The  
55 pseudopilus polymerisation is coupled to the secretion of substrates. The T2SS of *Dickeya*  
56 *dadantii* secretes more than 15 substrates, essentially plant cell wall degrading enzymes. In *D.*  
57 *dadantii*, the major pseudopilin or the major subunit of the pseudopilus is called OutG. To better  
58 understand the mechanism of secretion of these numerous substrates *via* the pseudopilus, we  
59 have been studying the structure of OutG by NMR. Here, as the first part of this study, we report  
60 the <sup>1</sup>H, <sup>15</sup>N and <sup>13</sup>C backbone and sidechain chemical shift assignment of the periplasmic domain  
61 of OutG and its NMR derived secondary structure.

## 62 **Biological context**

63 The type II secretion system (T2SS) is a molecular machinery which is widely used by  
64 Gram-negative bacteria to specifically secrete exoprotein substrates (Korotkov, Sandkvist and  
65 Hol, 2012; Thomassin *et al.*, 2017; Gu *et al.*, 2017). The substrates are species-specific and are  
66 often enzymes degrading biopolymers of carbohydrates, proteins, lipids and nucleotides  
67 (Cianciotto and White, 2017). In addition, T2SSs promote secretion of toxins, adhesins or  
68 cytochromes that are involved in respiration, motility or biofilm formation and remain attached  
69 to the bacterial cells (Nivaskumar and Francetic, 2014). The T2SS machinery is made up of  
70 twelve to fifteen components referred to as A to O, and spans both the inner and outer  
71 membrane. The T2SS could be divided into three functional blocks, the outer membrane pore  
72 composed of fifteen copies of the secretin D, the assembly platform comprising the inner  
73 membrane proteins F, L, M, C and the associated cytoplasmic ATPase E, which actively  
74 assembles a non-covalent polymer of protein subunits, called the pseudopilus, in the periplasm.  
75 The pseudopilus is composed of two types of proteins referred to as pseudopilins: the major  
76 pseudopilin G composing the bulk of the pseudopilus, and the minor pseudopilins H, I, J and K  
77 that form a complex initiating the pseudopilus formation (Nivaskumar and Francetic, 2014;

78 Escobar *et al.*, 2021). The minor pseudopilins are present in much lower abundance compared  
79 to the major pseudopilin but are crucial for the formation and stability of the pseudopilus and  
80 for secretion of substrates. Substrates are basically exported by the Sec or Tat translocator; are  
81 then folded in the periplasm where they are recruited by T2SS; with the elongation of the  
82 pseudopilus they reach the extracellular space through a secretin pore in the outer membrane  
83 (Korotkov, Sandkvist and Hol, 2012; Thomassin *et al.*, 2017; Gu *et al.*, 2017). It remains largely  
84 unknown how the growing pseudopilus can translocate the T2SS substrates and whether and  
85 how substrates are specifically recognized by pseudopilus.

86 *Dickeya dadantii* is a phytopathogenic  $\gamma$ -proteobacterium, which causes soft rot in  
87 vegetables and growing plants (Hugouvieux-Cotte-Pattat *et al.*, 2020). *D. dadantii* secrete more  
88 than 15 substrates *via* the T2SS (Kazemi-Pour, Condemine and Hugouvieux-Cotte-Pattat,  
89 2004). Most of the characterized substrates are hydrolytic enzymes that degrade the cell wall  
90 of plants and thereby release nutrients that the bacteria can take up and metabolise  
91 (Hugouvieux-Cotte-Pattat *et al.*, 2014). Occurrence of multiple, structurally dissimilar  
92 substrates makes *D. dadantii* an attractive model to study the mechanisms of T2SS.

93 In this study, we focused on the major pseudopilin from *D. dadantii*, named OutG, as  
94 an essential T2SS element. OutG is a 13.5 kDa protein composed of 153 residues. It has a short  
95 N-terminal prepilin signal sequence which allows correct insertion in the inner membrane, and  
96 is then cleaved by a prepilin peptidase. The mature protein OutG protein of 146 residues long  
97 is anchored in the inner membrane with an N-terminal, 24 residues long, hydrophobic  
98 transmembrane helix followed by a C-terminal globular domain of 122 residues located in the  
99 periplasm (thereafter termed to as OutGp).

100 Structural insight into OutG is of high importance for the understanding of the putative  
101 interactions of the pseudopilus with the substrates and other T2SS components. Here we present  
102 the resonance assignment and derived secondary structure of OutGp as a starting point for its  
103 structural and interaction studies by NMR.

## 104 **Method and experiments**

### 105 **Expression and purification of isotope labelled OutGp**

106 The pET20b(+) vector (*Novagen*) was used for the expression of OutGp in the  
107 *Escherichia coli* periplasm. The N-terminus of OutGp was successively fused to the PelB signal  
108 peptide, followed by 6His and the TEV cleavage site. The hybrid OutGp is exported by Sec  
109 translocon into the periplasm and the PelB signal peptide is cleaved off by the LepB signal  
110 peptidase. Thereafter, 6His tag was removed by TEV protease treatment during purification. In

111 this way, the final OutGp protein used in this study is composed of an N-terminal GMG  
112 sequence followed by residues M25 to P146 of the mature OutG (122 residues).  
113 Uniformly  $^{15}\text{N}$ - $^{13}\text{C}$  double-labelled OutGp was produced in M9 minimal media using 1 g/L of  
114  $^{15}\text{NH}_4\text{Cl}$  and 4 g/L  $^{13}\text{C}$ -glucose as the only nitrogen and carbon source, respectively. Protein  
115 production was induced by addition of 1mM IPTG overnight at 18°C in *E. coli* BL21 (DE3)  
116 cells. After induction the cells were lysed by sonication in equilibration buffer (50 mM Tris-  
117 HCl pH 8, 100 mM NaCl, 10mM Imidazole), then the polynucleotides were digested with  
118 nuclease (*Benzonase*®, *Sigma*) and the cell debris were pelleted by centrifugation at 16.000 g  
119 for one hour at 4°C. The supernatant was loaded onto a HiTrap HP column (*Cytiva*) previously  
120 loaded with  $\text{Ni}^{2+}$  ions, by saturating the resin with 0.1 M  $\text{NiSO}_4$  solution, then equilibrated in  
121 equilibration buffer. After loading of the lysate, the column was washed with the equilibration  
122 buffer, and bound proteins were eluted with a linear gradient of imidazole from 10 to 300 mM.  
123 The eluted protein fractions were pooled and treated with TEV protease overnight at 14°C, for  
124 the cleavage of the N-terminal His-tag. The mixture was loaded onto a HiTrap HP column  
125 (*Cytiva*) and the flow-through containing OutGp without its N-terminal His-tag was  
126 concentrated in a Vivaspin® 20 (*Satorius*) concentrator with a 5 kDa molecular weight cut-off.  
127 The concentrated OutGp fraction was loaded onto a Sephacryl S-100 column (*Cytiva*)  
128 equilibrated in 50 mM HEPES, pH 7, 100 mM NaCl, 5 mM  $\text{CaCl}_2$ . After elution, the fractions  
129 containing OutGp were pooled and concentrated to 0.43 mM for NMR data acquisition. The  
130 pH was adjusted to pH 6 by adding 2  $\mu\text{L}$  of HCl at 0.1M. All steps of the purification were  
131 evaluated by SDS-PAGE and in the final NMR sample no contaminants were visible in the  
132 final protein preparation subjected to NMR. All buffers used during the purification were  
133 supplemented with EDTA-free Protease inhibitor cocktail (*Roche*).

134

### 135 **NMR spectroscopy**

136 All NMR experiments were recorded on a 600 MHz Avance III HD (*Bruker Biospin*)  
137 or a 800 MHz Avance NEO (*Bruker Biospin*) spectrometer, both equipped with a cryogenically  
138 cooled triple resonance  $^1\text{H}$  [ $^{13}\text{C}$  /  $^{15}\text{N}$ ] probe. Standard set of experiments for the  $^1\text{H}$ ,  $^{15}\text{N}$  and  $^{13}\text{C}$   
139 for backbone and side chain resonance assignment were recorded at 25°C using NMR  
140 experiments implemented in TopSpin 3.6.1 and TopSpin 4.07 (*Bruker Biospin*) for the 600  
141 MHz and 800 MHz, respectively, and IBS libraries (Favier and Brutscher, 2019): 2D  $^1\text{H}$ - $^{15}\text{N}$   
142 HSQC,  $^1\text{H}$ - $^{13}\text{C}$  HSQC, HBCBCGCDHD, HBCBCGCDCEHE and 3D HNCA, HN(CO)CA,  
143 HNCACB, CBCA(CO)HN, HNCO, HN(CA)CO, HCCH-TOCSY, C(CO)NH-TOCSY,

144 H(CCO)NH-TOCSY, <sup>15</sup>N-NOESY and <sup>13</sup>C-NOESY. All proton chemical shifts were  
145 referenced to 2,2-dimethyl-2-silapentane-5-sulfonate (DSS) as 0 ppm. <sup>15</sup>N and <sup>13</sup>C chemical  
146 shifts were referenced indirectly to DSS (Wishart *et al.*, 1995). The data were analysed as  
147 previously described (Lopez-Castilla *et al.*, 2017) using CcpNMR Analysis (Vranken *et al.*,  
148 2005), and the prediction of the secondary structure was achieved by analysing the chemical  
149 shifts of HN, H $\alpha$ , C $\alpha$ , C $\beta$ , C', and N in TALOS-N (Shen and Bax, 2013).

150

### 151 **Extent of assignment and data deposition**

152 High quality data were obtained for OutGp as shown in the <sup>1</sup>H-<sup>15</sup>N HSQC spectrum in  
153 Fig 1. Backbone amide peaks were observed for all non-proline residues, except for the first  
154 three N-terminal residues (G22-G24). In total 96% of the observable backbone resonances and  
155 more than 91% of their corresponding sidechain resonances were assigned. Multiple backbone  
156 amide peaks of the C-terminal part of OutGp (N<sub>138</sub>GSNGNGNP<sub>146</sub>) were observed indicating  
157 that these residues have multiple conformations under the experimental conditions.  
158 Consequently, only one conformation of residues N138-N141 from this region could be  
159 assigned. It was not possible to assign any resonances corresponding to the last five residues  
160 (G<sub>142</sub>NGNP<sub>146</sub>), due to the repetitive nature of the sequence and the presence of a proline  
161 residue. The backbone amide peaks that could not be assigned are marked with red crosses in  
162 Fig 1. The chemical shift values have been deposited in the BioMagResBank  
163 (<http://www.bmrb.wisc.edu/>) under the accession number 51296.

164

### 165 **Secondary Structure**

166 The secondary structure of OutGp was estimated by using two approaches, secondary  
167 chemical shifts analysis and TALOS-N prediction (Fig. 2A). Secondary chemical shifts are  
168 obtained by calculating the differences between the assigned chemical shifts and the theoretical  
169 random coil chemical shift. The value of these secondary chemical shifts for C $\alpha$ , C $\beta$  and C'  
170 ( $\Delta\delta^{13}\text{C}\alpha$ ,  $\Delta\delta^{13}\text{C}\beta$  &  $\Delta\delta^{13}\text{C}'$ ) is related to the secondary structure of the individual residues.  
171 Positive values of  $\Delta\delta^{13}\text{C}\alpha$  and  $\Delta\delta^{13}\text{C}'$  correspond to a  $\alpha$ -helical conformation whereas negative  
172 values correspond to  $\beta$ -strand structure. For  $\Delta\delta^{13}\text{C}\beta$  positive values reflect  $\beta$ -strand structure  
173 and negative values  $\alpha$ -helical conformation (Fig. 2A).

174 To complete this prediction, a TALOS-N analysis of the assigned HN, H $\alpha$ , C $\alpha$ , C $\beta$ , C' and N  
175 chemical shifts was performed (Shen and Bax, 2013). The TALOS-N probabilities for each  
176 residue to be in an  $\alpha$ -helical conformation or a  $\beta$ -strand structure is plotted in Fig. 2B.

177 The results of both analysis methods agree to the location of the secondary structure elements,  
178 and reveal three helical segments ( $\alpha 1$ : K28-N54,  $\alpha 2$ : T60-Q62 and  $\alpha 3$ : G65-L67) and two  $\beta$ -  
179 strands ( $\beta 1$ : Q99-V101 and  $\beta 2$ : D110-S113), in the  $\alpha 1$ - $\alpha 2$ - $\alpha 3$ - $\beta 1$ - $\beta 2$  sequential order.  
180 Structural determination of OutGp will be performed following this study.

181

## 182 **Acknowledgements**

183 This work was funded by the Institut Pasteur, the Centre National de la Recherche Scientifique  
184 (CNRS), the French Agence Nationale de la Recherche (ANR Synergy-T2SS ANR-19-CE11-  
185 0020-01) and European Union's Horizon 2020 Research and Innovation program under the  
186 Marie Sklodowska-Curie Grant agreement no 765042. We thank Rémy Le Meur and Bruno  
187 Vitorge for their help in NMR experiments, and Olivera Francetic for helpful discussions. The  
188 800-MHz NMR spectrometer of the Institut Pasteur was partially funded by the Région Ile de  
189 France (SESAME 2014 NMRCHR grant no 4014526).

## 190 **References**

191

192 Cianciotto, N.P. and White, R.C. (2017) 'Expanding Role of Type II Secretion in Bacterial  
193 Pathogenesis and Beyond.' *Infect Immun* 85. <https://doi.org/10.1128/IAI.00014-17>

194

195 Escobar, C.A., Douzi, B., Ball, G., Barbat, B., Alphonse, S., Quinton, L., Voulhoux, R. and  
196 Forest, K.T. (2021) 'Structural interactions define assembly adapter function of a type II  
197 secretion system pseudopilin.' *Structure*. Oct 7;29(10):1116-1127.e8. doi:  
198 10.1016/j.str.2021.05.015.

199

200 Favier, A. and Brutscher, B (2019) 'NMRLib: user-friendly pulse sequence tools for Bruker  
201 NMR spectrometers', *Journal of Biomolecular NMR*, 73, pp. 199–211. doi: 10.1007/s10858-  
202 019-00249-1.

203

204 Gu, S., Shevchik, V.E., Shaw, R., Pickersgill, R.W. and Garnett, J.A. (2017) 'The role of  
205 intrinsic disorder and dynamics in the assembly and function of the type II secretion system.'  
206 *Biochim Biophys Acta Proteins Proteom* 1865:1255-1266. doi:10.1016/j.bbapap.2017.07.006.

207

208 Hugouvieux-Cotte-Pattat, N., Condemine, G., Gueguen, E. and Shevchik, V.E. (2020)  
209 'Dickeya Plant Pathogens.' in *eLS*, John Wiley & Sons, Ltd (Ed.). pp 1-10

210

211 Hugouvieux-Cotte-Pattat, N., Condemine, G., and Shevchik, V. E. (2014) 'Bacterial pectate  
212 lyases, structural and functional diversity.' *Environmental microbiology reports* 6, 427-440 doi:  
213 10.1111/1758-2229.12166.

214

215 Kazemi-Pour, N., Condemine, G. and Hugouvieux-Cotte-Pattat, N. (2004) 'The secretome of  
216 the plant pathogenic bacterium *Erwinia chrysanthemi*', *Proteomics*, 4(10), pp. 3177–3186. doi:  
217 10.1002/pmic.200300814.

218



219 Korotkov, K. V., Sandkvist, M. and Hol, W. G. J. (2012) ‘The type II secretion system:  
220 Biogenesis, molecular architecture and mechanism’, *Nature Reviews Microbiology*, pp. 336–  
221 351. doi: 10.1038/nrmicro2762.  
222

223 López-Castilla, A. *et al.* (2017) ‘<sup>1</sup>H,<sup>15</sup>N and<sup>13</sup>C resonance assignments and secondary  
224 structure of PulG, the major pseudopilin from *Klebsiella oxytoca* type 2 secretion system’,  
225 *Biomolecular NMR Assignments*, 11(2), pp. 155–158. doi: 10.1007/s12104-017-9738-7.  
226

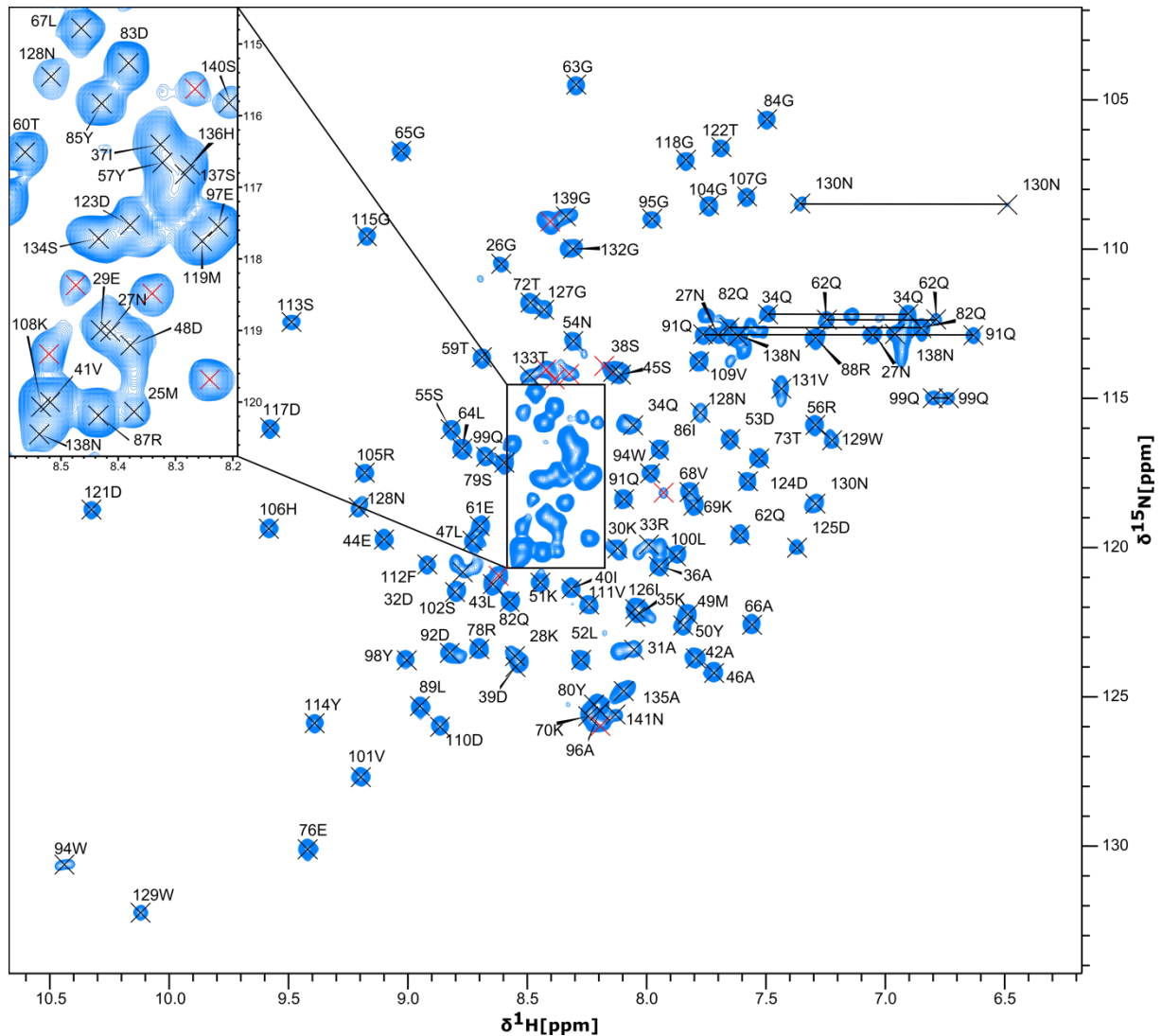
227 Nivaskumar, M. and Francetic, O. (2014) ‘Type II secretion system: A magic beanstalk or a  
228 protein escalator’, *Biochimica et Biophysica Acta - Molecular Cell Research*. Elsevier B.V.,  
229 1843(8), pp. 1568–1577. doi: 10.1016/j.bbamcr.2013.12.020.  
230

231 Shen, Y. and Bax, A. (2013) ‘Protein backbone and sidechain torsion angles predicted from  
232 NMR chemical shifts using artificial neural networks’, *Journal of Biomolecular NMR*, 56(3),  
233 pp. 227–241. doi: 10.1007/s10858-013-9741-y.  
234

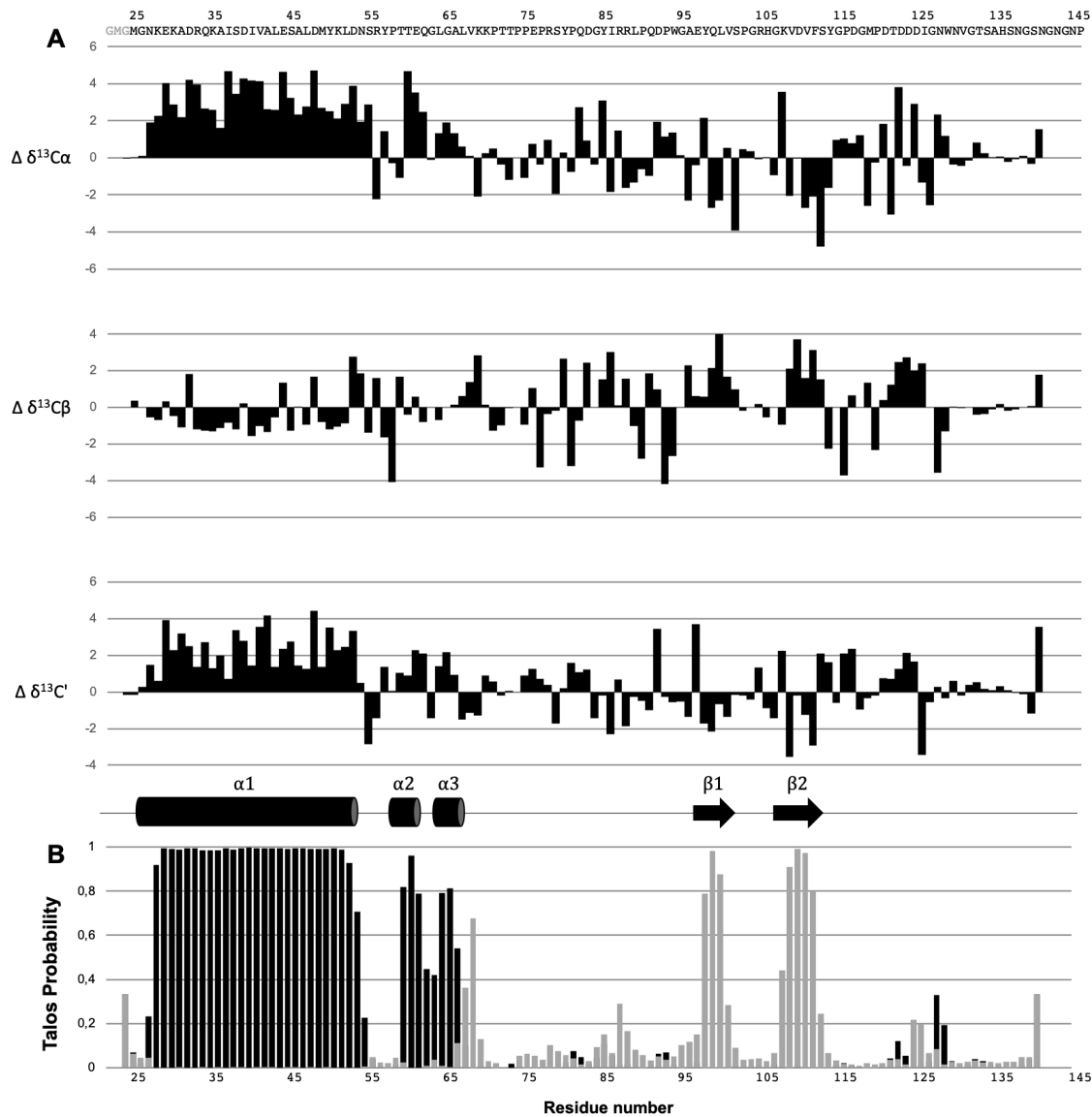
235 Thomassin, J.L. *et al* (2017) ‘The trans-envelope architecture and function of the type 2  
236 secretion system: new insights raising new questions. *Mol Microbiol* 105:211-226. doi:  
237 10.1111/mmi.13704.  
238

239 Vranken, W. F. *et al.* (2005) ‘The CCPN data model for NMR spectroscopy: Development of  
240 a software pipeline’, *Proteins: Structure, Function and Genetics*, 59(4), pp. 687–696. doi:  
241 10.1002/prot.20449.  
242

243 Wishart, D. S. *et al.* (1995) ‘<sup>1</sup>H, <sup>13</sup>C and <sup>15</sup>N chemical shift referencing in biomolecular  
244 NMR’, *Journal of Biomolecular NMR*, 6.  
245  
246  
247  
248

250  
251

252 Fig. 1-  $^1\text{H}$ - $^{15}\text{N}$  HSQC spectrum of OutGp, major pseudopilin of *Dickeya dadantii*, recorded on  
 253 a sample of 0.43 mM protein in 50 mM HEPES pH 6, 100 mM NaCl, 5 mM  $\text{CaCl}_2$ , 5%  $\text{D}_2\text{O}$   
 254 (v/v), at 25°C on a 600 MHz Avance III HD (*Bruker Biospin*) spectrometer. The resonance  
 255 assignment for the backbone amide peaks are displayed using sequence number and one letter  
 256 amino acid code. The red crosses indicate backbone amide peaks which could not be assigned  
 257 and corresponding to the region  $\text{G}_{142}\text{NGNP}_{146}$ .  $\text{NH}_2$  peaks of Asn and Gln sidechains are  
 258 connected by horizontal lines.



259

260 Fig. 2 – Secondary structure prediction based on the chemical shifts of OutGp.

261 **A** Secondary chemical shifts of  $C\alpha$ ,  $C\beta$  and  $C'$  resonances. The sequence of OutGp is shown  
 262 at the top. **B** TALOS-N secondary structure probabilities were used to predict the secondary  
 263 structure elements along the protein sequence. The probability for each residue to be in an  $\alpha$ -  
 264 helical conformation (black bars) or in  $\beta$ -sheet conformation (grey bars) are plotted as a  
 265 function of residue number. Both the secondary chemical shifts and TALOS-N secondary  
 266 structure prediction agree to a consensus of secondary structure elements illustrated between  
 267 panel A and B (cylinders represent  $\alpha$ -helices and arrows represent  $\beta$ -sheets).